



Design, development and performance analysis of FSPV system for powering sustainable energy based mini micro-grid

Sagnik Bhattacharya¹ · Anik Goswami^{1,2} · Pradip Kumar Sadhu¹

Received: 30 September 2022 / Accepted: 18 April 2023 / Published online: 21 April 2023
© The Author(s), under exclusive licence to Springer-Verlag GmbH Germany, part of Springer Nature 2023

Abstract

The Floating Solar Photovoltaic System (FSPV) is emerging as a favorable technology to policymakers for economically harvesting renewable energy. The implementation of large-scale photovoltaic (PV) systems is often disrupted due to the unavailability of land. The FSPV systems, where the PV modules are floated in water bodies facilitate optimal utilization of water resources and land assets. The FSPV provides higher power output compared to land-based PV systems of the equal area because of improved energy conversion efficiency at a lower temperature. Another opportunity for the FSPV system is integration with hydropower stations, storage systems, and the electric grid. This paper explores the flood duration curve-based optimal sizing of the FSPV System with the objective of electrification of rural micro-grid. A comparison of energy output and module temperature rise has been made for the FSPV system and its equivalent land-based PV system of equal area. The system generates 18.08 GWh, which is 10.04% more than the land-based PV system. The DC Capacity factor is 17.2%. The Demand Supply Factor (*DSF*) for a particular day in winter, spring, summer, and monsoon is 37.55%, 41.7%, 45.9%, and 25% respectively. The results indicate that the FSPV system is a sustainable alternative to power renewable energy-based mini micro-grid and provide cost effective electricity to all.

1 Introduction

The energy demand in the world is continuously increasing. With rising population and increase in per capita energy consumption, the government is seriously concerned about energy security.

Especially in 2021, the world saw a 6% increase in electricity demand (over 1500 TWh) primarily due to economic recovery from covid-19 pandemic; accompanied by unforeseen weather-related events such as colder-than-average winter and hotter summer. This resulted in serious fuel and power shortages worldwide in the first half of 2021. Simultaneously the environmental impacts of

conventional fossil fuels and extreme weather conditions due climate change has emphasised the need for sustainable development in the electricity sector. In 26th Conference of Parties (COP26) more than 50 countries including European Union have committed for net zero greenhouse gas emission (IEA 2021). Renewable Energy Sources (RES) like wind, solar photovoltaic (PV) and small-scale hydropower are instrumental for meeting the energy demand of the future as well as fulfilling the net zero emission targets. Net capacity addition of renewable energy is expected to exceed 300 GW in 2022; PV installations being the largest share in terms of technology (IEA 2022).

As on 2021, the worldwide installed capacity of PV was 843,086 MW (IRENA 2022). For rural electrification, the PV based micro-grids are recognised to have positive economic and social impacts that improve the standard of living in remote areas (Tsai et al. 2021). PV systems, when coupled with other renewable sources like wind or hydroelectric plants improve system reliability and economy. Goswami et al. (2020) proposed a solar-wind hybrid system for electrification of a remote island in Sunderban. The levelized cost of electricity was found to be lower than the grid electricity of the area. Solar PV systems, by the virtue

✉ Sagnik Bhattacharya
sagnik.bhattacharya15@gmail.com

Anik Goswami
anik91_go@rediffmail.com

Pradip Kumar Sadhu
pradip_sadhu@yahoo.co.in

¹ Department of Electrical Engineering, Indian Institute of Technology (ISM), Dhanbad 826004, India

² University of Engineering and Management, Kolkata 700160, India

to its scalability find diverse applications as ground mounted, roof-top PV, Building-Integrated-PV and FSPV systems. As the sizes of roof-top PV and BIPV systems are constrained by the building architecture, policymakers have relied on the ground mounted PV systems for PV capacity addition on large scale (IRENA 2019).

However, unavailability of land for large scale PV installation is a major issue for countries with a large population density. If the installation is based solely on maximisation of PV generation potential, agricultural land, forest and biodiversity would be heavily impacted, which in turn contribute to environmental degradations and increment in carbon-emission (Kiesecker et al. 2019). A study on EU, India, Japan and South Korea indicated that land-based PV system at 25 to 80% energy mix will occupy 0.5 to 5% of the total land area by 2050. The corresponding change in land cover result an emission of up to 50 g CO₂ per kWh electricity generation (Van de Ven et al. 2021). The current PV technology converts nearly 20% of solar energy to electricity; the rest amount is dissipated as heat energy to the ambient. Large-scale land-based PV installations cause Photovoltaic Heat Island (PHI) effect, due to lack of thermal regulation. With PV installations in proximity to residential areas, PHI might contribute to the Urban Heat Island (UHI) effects that increase the local temperature (Barron et al. 2016). Land based PV systems are impacted by non-uniform shading conditions caused by neighbouring trees, civil constructions (buildings and towers), soiling and dust. This results in higher mismatching losses in the array that reduces output power generation and creates multiple peaks in power-voltage and current–voltage characteristics that puts the conventional Maximum-Peak-Power-Tracking (MPPT) systems in challenging situation (Yadav and Mukherjee 2021).

Floating Solar Photovoltaic (FSPV) systems overcome the limitations of land-based utility scale PV installations. The PV panels are kept on a structure floating over the water-bodies such as artificial reservoirs, estuary and ocean, lakes, mining pit, water treatment plants etc. Spencer et al. (2018) presented the opportunity of FSPV systems on man-made reservoirs. The FSPV design and installation is easier on such reservoirs due to availability of accurate bathymetric data. The FSPV plants installed on the reservoirs previously made for irrigation and hydroelectric generation; has opportunities to integrate with main grid as well as to the pumped storage plants. Such hybrid systems provide better energy security with increased generation capacity and better hydropower generation due to reduction of evaporation loss (Gonzalez et al. 2021). Ravichandran and Panneerselvam (2021) evaluated an FSPV system of 5 MW capacities on an artificial reservoir in India. The FSPV provides annual electricity of 160 GWh and saves 1.4 million cubic meters of water by reducing

evaporation losses. Lee et al (2020) estimated a global generation potential of 10,616 TWh for FSPV integrated hydropower systems. Shyam et al. (2022) explored the integration of small scale FSPV system with a pumped-storage hydroelectric plant.

In FSPV system the land-energy conflicts (electricity generation vs. agricultural use of land) are avoided by optimal utilization of land assets and water resources. For FSPV systems, the cost for land acquisition and site preparation is drastically reduced (Goswami et al. 2019). Makhjia et al. (2021) proposed the off-grid FSPV system for electrification of a remote area in Chhattisgarh where grid extension would have caused deforestation and more right of way cost. Moreover, the losses due to shading and soiling in FSPV are lesser than that of land-based PV. Hafeez et al. (2022) identified two key benefits of FSPV on urban lakes, firstly avoidance of land-acquisition costs and lesser maintenance cost due to reduced soiling. The FSPV system has higher energy output compared to land-based PV systems with equal area and equal solar irradiation. Liu et al. (2017) estimated the improvement in efficiency of floating solar cell as 1.58 to 2% compared to terrestrial solar cell in Chinese climatic conditions. In Norway, 5% to 6% higher yield due to evaporative cooling of FSPV system is reported by Kjeldstad et al. (2021). The points of concern that prevents the widespread development of FSPV system are lack of exhaustive guidelines for installation, proper design analysis, economic operation, maintenance of FSPV system and regulatory barriers regarding water rights (Gadzanku et al. 2021).

This paper presents a design analysis and optimal sizing methodology for a FSPV system installed on a reservoir addressing the above issues, to power a mini micro-grid in India. The salient features of this work are as follows:

1. Selection of site for micro-grid through a diligent analysis of power supply–demand scenario, penetration of renewable energy resources in the grid, population size and per capita consumption of electricity.
2. Application of historical data of daily reservoir water level and capacity to obtain Flood Duration Curve (FDC).
3. Based on the FDC the area available for the FSPV plant is chosen from the capacity-area table.
4. Performance analysis of FSPV system in System Advisor Model (SAM) software, corresponding to weather data from National Solar Radiation Database.
5. Comparison of FSPV and the equivalent land-based PV system in terms annual and monthly power generations, capacity utilization factor, load factor, module temperature.
6. Calculation of energy-based metrics such as yield factor, performance ratio, probability distribution of

module temperature and power output, renewable energy fraction and demand supply factor.

- Seasonal variation and hourly variation of the FSPV system output is also taken into account and discussed against hourly load-curve of the study area.

2 Mathematical modelling

2.1 Modelling of PV cell

The photovoltaic (PV) cell is the smallest unit of PV system. It is essentially a PN junction which generates electricity when light is incident on it. The basic equivalent circuit of PV cell is modelled after a controlled current source in parallel with a diode, along with series resistance (R_S) and shunt resistance (R_P) as given by Fig. 1 (Villalva et al. 2009). The series resistance R_S is the sum of contact resistance between P layer and N layer and resistances between each of the layers and the metal frames. It has a low value. The shunt resistance R_P is modelled to simulate the effect of leakage currents and the resistances are of higher order.

The current of PV cell is the algebraic sum of the diode current (I_d) and photocurrent (I_{PV}). The value of the controlled current source (I) and diode current (I_d) are given by Eq. 1 and Eq. 2 respectively

$$I = I_{PV} - I_d - \frac{V + R_S I}{R_P} \tag{1}$$

$$I_d = I_0 \left(e^{\frac{(V+R_S I)}{aV_t}} - 1 \right) \tag{2}$$

where I_{PV} is the current generated due to photoelectric effect, I_d is the diode current, I_0 is the diode saturation current flowing in the reverse direction due to thermally generated carriers. Here a is the degree of ideality of the diode which is a constant between 1 and 1.5. Here V is the voltage across the cell and V_t is the thermal voltage of a cell given by Eq. 3.

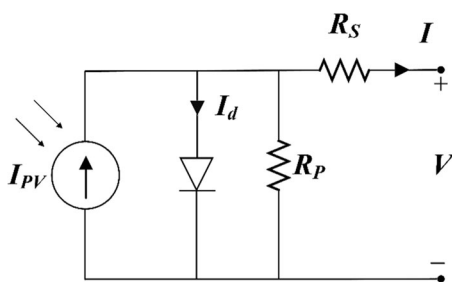


Fig. 1 The equivalent circuit of a PV cell

$$V_t = \frac{kT}{q} \tag{3}$$

where k is the Boltzmann constant 1.38×10^{-23} J/K, q is the charge of electron (1.602×10^{-19} C) and T is the temperature in kelvin. The photovoltaic current as a function of irradiance (L) and temperature (T_c) is given by Eq. 4. The difference between cell temperature (T_c) and reference temperature (T_{ref}) is termed as ΔT in Eq. 5

$$I_{PV} = (I_{PVref} - K_I \Delta T) \frac{L}{L_{ref}} \tag{4}$$

$$\Delta T = T_c - T_{ref} \tag{5}$$

Here I_{PVref} is the nominal value of photocurrent at standard temperature condition (STC) and standard irradiation L_{ref} . The temperature dependence of diode saturation current (I_0) at the cell temperature (T_c) is shown in the Eq. 6

$$I_0(T) = I_{0ref} \left(\frac{T_c}{T_{ref}} \right)^3 e^{\frac{qE_g}{ak} \left(\frac{1}{T_{ref}} - \frac{1}{T_c} \right)} \tag{6}$$

Here E_g is the energy band-gap in eV, and a denotes the diode ideality factor. The variation of open circuit voltage with respect to temperature (T) is given by Eq. 7.

$$V(T, L) = V_{Tref, Lref} + \mu_V (T - T_{ref}) \tag{7}$$

Here $V_{Tref, Lref}$ is the open circuit voltage at standard temperature T_{ref} and irradiance L_{ref} and μ_V is the temperature coefficient of voltage in V/°C. The overall current from the PV cell is dependent on irradiance and temperature as in Eq. 8.

$$I(T, L) = I_{Tref, Lref} \left(\frac{L}{L_{ref}} \right) + \mu_I (T - T_{ref}) \tag{8}$$

Here $I_{Tref, Lref}$ is the current at standard temperature T_{ref} and irradiance L_{ref} and μ_I is the temperature coefficient of current in A/°C. The power output at a temperature T and irradiance L is given by Eq. 9.

$$P(T, L) = V(T, L) \times I(T, L) \tag{9}$$

A PV module with N_S string and N_M cells per string is modeled by from Eq. (1) and Eq. (2). The output current (I_m) is expressed as in Eq. (10). Here the thermal voltage of a module with N_M cells per string is denoted by V_{tm} as shown in Eq. (11). The equivalent series resistance (R_{SEq}) and shunt resistance (R_{PEq}) are expressed as in Eq. (12) and Eq. (13).

The Eq. (8)–(10) indicates the power generated by a PV module increases with irradiance and decreases at higher module temperature.

$$I_m = N_S I_{PV} - N_S I_0 \left\{ e^{\left(\frac{V_m + R_{SEq} I_m}{a V_{im}} \right)} - 1 \right\} - \left(\frac{V_m + R_{SEq} I_m}{R_{PEq}} \right) \tag{10}$$

$$V_{im} = \frac{N_M k T}{q} \tag{11}$$

$$R_{SEq} = \frac{N_M}{N_S} \times R_S \tag{12}$$

$$R_{PEq} = \frac{N_M}{N_S} \times R_P \tag{13}$$

2.2 Temperature dependence of efficiency

The energy conversion efficiency (η) of PV cell depends on the cell temperature. The efficiency (η) is expressed in Eq. 14 in terms of open circuit voltage (V_{OC}), short circuit current (I_{SC}), fill factor (FF) and incident solar irradiation (P_{in}). (Solanki 2015)

$$\eta = \frac{V_{OC} I_{SC} FF}{P_{in}} \tag{14}$$

While the increase in I_{SC} due to rise in cell temperature is negligible, both V_{OC} and FF decreases with temperature. The rate of change of open circuit voltage with temperature is derived by Green (1982) as shown in Eq. 15.

$$\frac{dV_{OC}}{dt} = -\frac{1}{T} \left(\frac{E_g}{q} - V_{OC} + \gamma \frac{kT}{q} \right) \tag{15}$$

Here, γ is the exponent to express the temperature dependence of reverse saturation current (I_0). It has a value between 1 and 3. Since the potential corresponding to energy band gap (E_g/q) is always greater than the open circuit voltage (V_{OC}), the rate of change of open circuit voltage with cell temperature is always negative. For silicon wafer-based cells, the decrease in V_{OC} due to higher temperature causes a reduction of 0.4–0.5% reduction in power output per °C. At modular level, the first order approximation of energy conversion efficiency (η) as a function of temperature (T_m, T_{ref}) is shown in Eq. 16

$$\eta = \eta_{ref} \{ 1 - \beta (T_m - T_{ref}) \} \tag{16}$$

For crystalline silicon, the temperature coefficient (β) is 0.0045 °C⁻¹. Here η_{ref} denotes the efficiency at reference temperature T_{ref} . Therefore, a reduction in module temperature improves the efficiency of PV system.

The empirical relation between the module temperature (T_m) and ambient temperature (T_a) as a function of irradiance (L) and wind speed (U_w) as shown in Eq. 17 (Prilliman et al. 2020).

$$T_m = L e^{(a+U_w b)} + T_a \tag{17}$$

The parameters a and b are adjusted for different materials and mounting structures.

Wang et al. (2020) utilised the physics-based model for convective heat transfer for analysis of PV module under practical outdoor condition. Alktrane and Bencs (2022) presented the evaporative cooling effect on PV module due to convective heat transfer. The heat transfer due to convection (Q) is shown in Eq. 18

$$Q = h A_m (T_m - T_a) \tag{18}$$

Here, the area of the PV module is A_s and the heat transfer coefficient is denoted by h . This coefficient depends on thermal conductivity of air (K_A) and inversely proportional to the characteristic length (l_{Ch}) of the FSPV module as shown in Eq. 19. The characteristic length is the ratio of module area to perimeter as described in Eq. 20.

$$h = \frac{N_u K_A}{l_{Ch}} \tag{19}$$

$$l_{Ch} = \frac{A_m}{P} \tag{20}$$

Here N_u denotes the Nusselt number that depends on the nature of air flow. The value increases from laminar flow to turbulence flow. Therefore, a linear relation between coefficient of convective heat transfer (h) and wind speed (U_w) can be expressed as in Eq. 21

$$h = c + d U_w \tag{21}$$

Liu et al (2017) considered the coefficients c and d as 8.55 and 2.56 respectively. The wind speed U_w is higher in case of water bodies compared to land. Moreover, evaporative cooling reduces the ambient temperature of water bodies. The cumulative effect lowers the module temperature. This temperature regulation due to evaporative cooling helps to increase the energy conversion efficiency and other performance parameters for FSPV systems.

2.3 Performance analysis

The installable PV capacity (P_c) in terms of the incident solar irradiation converted to electricity is given by Eq. 22.

$$P_c = \eta \times L \times A_{real} \tag{22}$$

Here η is the efficiency of solar PV array, A_{real} is available module area in m², and L is the solar irradiation in Watts/m². However, for an AC network the losses in the inverter would reduce the output. Further the effect of module temperature (T_m) is neglected in Eq. 22. A more practical expression of the output power for the PV system (P_{PV}) is given by Eq. 23.

$$P_{PV} = \eta \eta_{PV} \eta_{inv} A_m L (1 - \alpha_p [T_m - T_{ref}]) \tag{23}$$

Here n is the number of PV modules. The rated module efficiency and inverter efficiency are denoted by η_{PV} and η_{inv} respectively. A_m is the area of one module in m^2 . L is the solar irradiation in $Watts/m^2$. T_c is the module temperature in $^{\circ}C$ and T_{ref} is standard operating temperature $^{\circ}C$. Here α_p is the temperature coefficient of power in $\%/^{\circ}C$.

The energy yield (Y_E) is defined as the ratio of energy output of the FSPV system divided by the installed system capacity, given by Eq. 24.

$$Y_E = \frac{E_G}{P_{in}} \tag{24}$$

where E_G is the annual electricity generation in kWh and P_{in} is the installed capacity in kW. The performance ratio PR is given by the Eq. 25 where Y_{ef} is the final yield and Y_{er} is the reference yield. The final yield (Y_{ef}) is defined in Eq. 26 as the ratio of total AC energy output (E_{ac}) of the system in kWh by the maximum rating of the system (P_c) in kW. The reference yield defined in Eq. 27 the ratio of incident solar irradiance on the PV panel area (E_L) in kWh/ m^2 to irradiance at STC (L_{STC}) in kWh/m^2 .

$$PR = \frac{Y_{ef}}{Y_{er}} \tag{25}$$

$$Y_{ef} = \frac{E_{ac}}{P_c} \tag{26}$$

$$Y_{er} = \frac{E_L}{L_{STC}} \tag{27}$$

The Capacity Utilization Factor (CUF), Average Load ($P_{L_{avg}}$) and Load Factor (LF) are given by Eq. 28, Eq. 29 and Eq. 30 respectively

$$CUF = \frac{E_S}{365 \times 24 \times P_C} \times 100 \tag{28}$$

Here E_S is the amount of energy in MWh supplied by the FSPV plant in one year, and P_C is the installed capacity of the FSPV plant in MW.

$$P_{L_{avg}} = \frac{E_D}{365 \times 24} \tag{29}$$

$$LF = \frac{P_{L_{avg}}}{P_{L_{max}}} \times 100 \tag{30}$$

Here E_D is the annual electricity demand in kWh, $P_{L_{avg}}$ is the average load in kW and $P_{L_{max}}$ is the maximum electricity demand at a given time.

The annual Demand Supply Factor (DSF_{annual}) and the RES Fraction (F_r) is defined by Al-Ghussain et al. (2020) as in Eq. 31 and Eq. 32

$$DSF_{annual} = \frac{H}{365 \times 24} \tag{31}$$

$$F_r = \frac{D_H}{D} \tag{32}$$

Here H is the number of hours in a year when the generation by FSPV system would be sufficient to meet the energy demand. The D_H and D indicates the demand covered by renewable energy sources, and the energy demand at that time in kWh respectively. The Demand Supply Factor (DSF_{day}) calculated for a day is calculated by Eq. 33 based on the number of hours in a day when energy system caters the complete load demand (H_D).

$$DSF_{day} = \frac{H_D}{24} \tag{33}$$

3 Methodology

3.1 Site selection

India has a phenomenally diverse electricity sector with different levels of consumers and ever-increasing demand. The future of clean and renewable energy installation is bright, as India has pledged to increase non-fossil fuel capacities that would meet 50% of the power demand and reduce the carbon intensity by 45% by 2030 (IISD 2020). The Indian power grid is divided into five regions: Northern, Eastern, Southern, Western, and North-Eastern. Lack of RES installations of eastern grid compared to southern and western grids of India is one of the key issues identified by Nag and Sarkar (2018). The eastern region, despite having large geographic area and increasing population, has only 10.92% of the nation-wide new installation capacity as on April 2022. The entire eastern region including Jharkhand has the highest share of coal based thermal power plants; 81.94% of installed capacity as shown in Fig. 2 (CEA 2022). Among the states of eastern

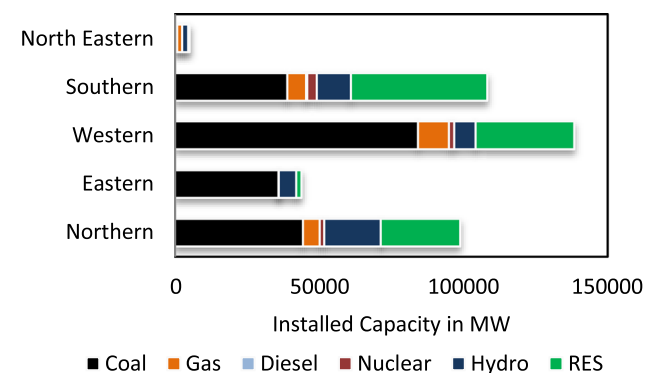


Fig. 2 Installed capacity of renewable energy in different regions of India as on April 2022

region, Jharkhand has the lowest share of renewable energy generation (0.6%) in last ten years as given by Fig. 3.

Jharkhand has an installed capacity of coal based thermal power of 4250 MW, hydropower of 210 MW and RES of 97.14 MW. The renewable energy mix in the installed capacity is 2.14%. Per capita electricity consumption is lesser than the national average although it became double in 18 years (CEA 2020) as given by Fig. 5. In addition, Jharkhand has experienced a peak shortage of power supply in recent years. A shortage of 102 MW was observed in January 2021 (6% of the peak demand). Between April 2021 and February 2022, the amount of energy not supplied was 454 MU, nearly 4.5% of the energy requirement (CEA 2022). Keeping in mind, the rising population and per capita consumption of electricity, this state has a remarkable scope of expansion in renewable power generation and phasing down the coal based thermal power plants.

The Panchet town and nine nearby villages in the Nirsa and Chirkunda block of Jharkhand are chosen to form the FSPV based micro-grid as shown in Fig. 4.

The demographic analysis of the study area based on 2011 census data indicates that the socio-economic conditions are lower than the national average. The working population is 39.9% of the total population, among which 41.75% are the marginal workers. Agricultural labour and household based productions are major sources of income. The proposed micro-grid would contribute to the quality of lives of the residents in the following ways.

1. Reliable and affordable electricity would increase the hours of commercial activities like markets, small industries, irrigation and agricultural processing (Agrawal et al. 2019). This would increase the human development index (HDI) of the area.
2. Uninterrupted electricity in hospitals, medicine stores and health centres would improve the health security in the area. In the households, dependence on kerosene and diesel generators would be eliminated.

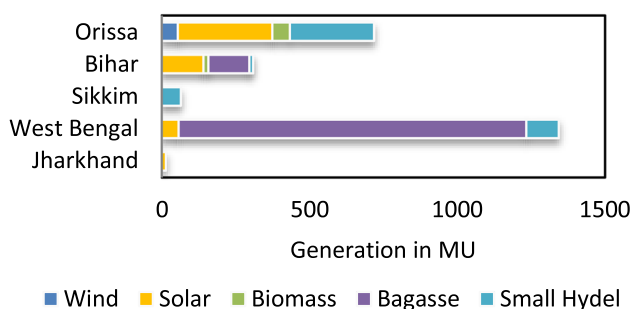


Fig. 3 Renewable energy generation from 2012 to 2022 the states of eastern region



Fig. 4 Satellite view of Panchet town and nearby villages

3. Affordable electricity would increase the study hours for students, provide better access to internet and communication systems, thus improving the literacy rate as well as the standards of living (Tsai et al. 2021).

The Panchet Reservoir in the district of Dhanbad, Jharkhand, India is chosen as the site for FSPV installation. It is located in the upstream of the confluence of Damodar River with Barakar River. The reservoir has a water spread of 28.48 km² at the dead storage level (elevation from mean sea level of 119.48 m) and 59.56 km² at the normal pool level (elevation from mean sea level of 125.0 m) (Precision Survey Consultancy 2020).

3.2 Data collection

The meteorological data downloaded from National Solar Radiation Database was used for estimation of energy generation by the FSPV system. The electricity demand in Panchet and its neighbourhood area is estimated from the 2011 census data.

3.2.1 Estimating available area of FSPV:

For Panchet Reservoir, the daily reservoir level & storage time series data for period 2016 to 2022 was obtained from National Water Informatics Centre. The area was estimated from the area-capacity curve and capacity-area table in “Sedimentation Survey Report of Panchet Reservoir under NHP” (2020) prepared by Precision Survey Consultancy. Some important specifications of the reservoir are presented in the Table 1.

Table 1 Details of panchet reservoir

Category	Data
State	West Bengal
District	Purulia
Minimum level of water	118.99 m (Elevation from Mean Sea Level)
Maximum level of water	131.24 m (Elevation from Mean Sea Level)
Full Reservoir level (FRL)	124.97 m
Minimum storage in BCM in 6 years	0.005
Maximum storage in BCM in 6 years	0.184
Live capacity at FRL in BCM	0.184
Dead storage level (m) above MSL	119.48
Flood management level (m) above MSL	124.97 m
Dead storage in MCM	169
Max. utilizable Flood Management level (m) above MSL	132.58
Flood management storage MCM	434

3.2.2 System simulation data

For the sizing of FSPV system, the hourly time-series data of solar irradiance, temperature, wind speed was obtained from National Solar Radiation Database. A correction was performed in temperature and wind speed to simulate the cooling effect of water bodies on the performance of FSPV systems. Summary of the weather data is presented in Table 2.

The micro-grid load was considered in terms of population size of Panchet and nine nearby villages. The population data as per as 2011 census is presented in Table 3.

Assuming 1% annual growth in population, the population in 2021 is estimated to be 22,404. The per capita annual electricity consumption of Jharkhand is reported to be 835 kWh in 2019–2020 and nearly 900 kWh for last five years Fig. 5. The rural load of the selected area is expected to be 80% of the average, which amounts to a 700 kWh per capita annual electricity consumption. Therefore, a requirement of 15,682.8 MWh system is estimated. A typical daily load curve for rural Jharkhand is determined by Nag et al. (2018). A scaled version of such daily load curve is presented in Fig. 6

Table 3 Population data in Panchet and nearby villages

Panchet Town and Nearby Villages	Population in 2011 Census
Panchet	7296
Ledaharia	2115
Shanmara	2483
Rangametya	1402
Talberya	999
Raghunathpur alias Nepura	403
Baidyanathpur	529
Labsan	32
Benagaria	2667
Paltabari	2356
Total	20,282

3.3 Sizing of floating PV system

The optimal area for FSPV system is estimated using the methodology proposed by Reges et al. (2022). The methodology uses Flood Duration Curves (FDC) to ensure the water level in a certain area of reservoir remains above a sufficient value for a certain percentage of time in the entire year. The FDC regarding the water-level indicates

Table 2 Location details

Categories	Data
Latitude	23.65°N
Longitude	86.75°E
Global horizontal irradiance	5.17 kWh/m ² /day
Direct normal (Beam) irradiance	3.84 kWh/m ² /day
Diffuse horizontal irradiance	2.43 kWh/m ² /day
Average temperature	26.1 °C (For Land Data); 18.2 °C (For Water data)
Average wind speed	0.1 m/s (For Land Data); 0.2 m/s (For Water Data)

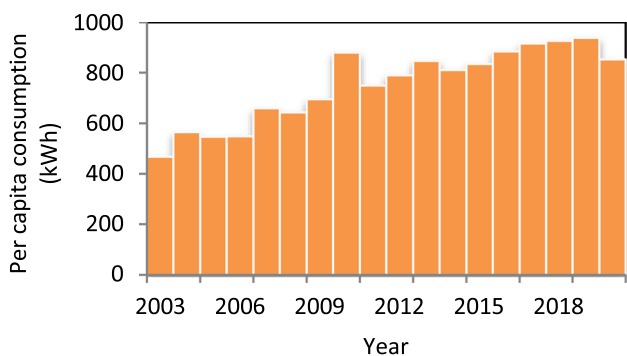


Fig. 5 Annual per capita electricity consumption of Jharkhand (CEA 2020)

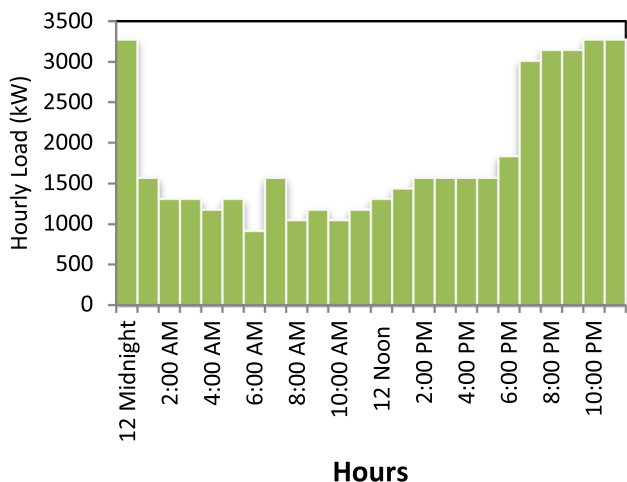


Fig. 6 Typical daily load curve for rural Jharkhand, presented by Nag et al. (2018); scaled to match the estimated annual load demand of Panchet and nearby villages

the requirement of anchoring and mooring for FSPV pontoon. The FDC regarding the area indicates the maximum area available for FSPV structures during hot dry seasons. By utilizing, the daily reservoir level & storage time series data collected for 6 years the FDC curves in terms of water level i.e., elevation above Mean Sea Level and Reservoir capacity in Billion Cubic Meter (BCM) are created as shown in Fig. 7 and Fig. 8 respectively.

The Fig. 7 indicates that the for 80% of the time the fluctuation of water level is 3 m i.e., between 122 and 125 m above mean sea level (MSL). As the full reservoir level of the dam is designed to have an elevation above MSL of 125 m, the design of mooring and anchoring requires to accommodate 3 m of fluctuation. From these curves, 80% reliability level is chosen to determine the available area for FSPV. The Fig. 8 indicates that the reservoir area of 40 km² is available for 80% duration, 1% of that area is considered for the entire floating structure.

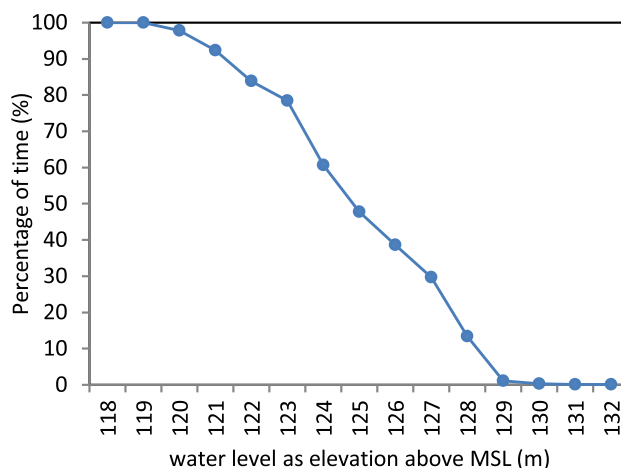


Fig. 7 Flood Duration Curve in terms of reservoir water level as elevation above the mean sea level (NWC 2022)

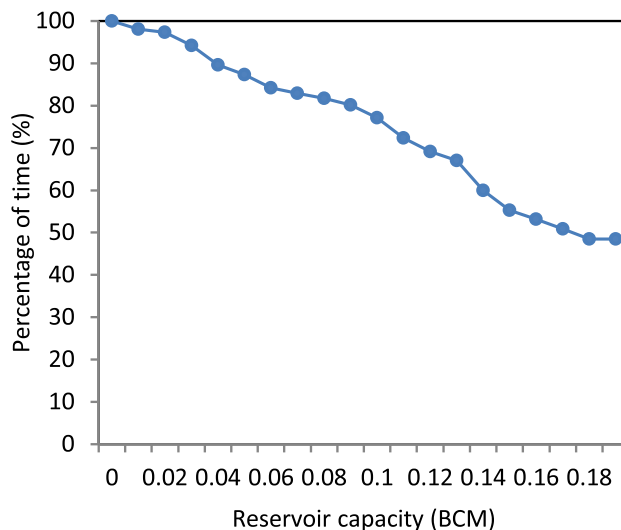


Fig. 8 Flood Duration Curve in terms of reservoir water capacity in BCM (NWC 2022)

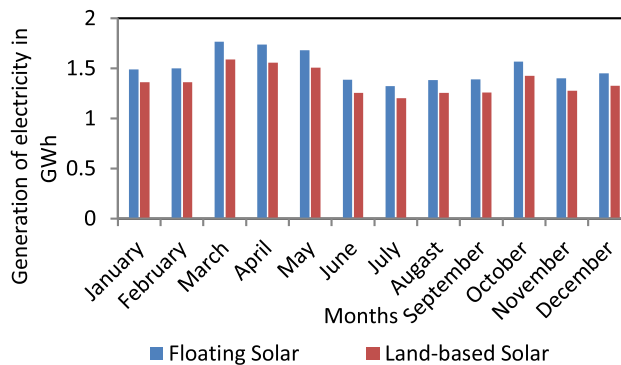


Fig. 9 Monthly energy generation by FSPV and equivalent Land-based PV system

4 Design and simulation

For Simulation, the parameters considered in SAM are presented in Table 4. For floating systems, the losses due to soiling, shading and mismatch are considered to be less than the land-based PV systems. Also, the temperature value from the weather data file is scaled down in a way such that the temperature difference between land and water remains 8 °C to 10 °C in summer days and 2 °C to 4 °C in winter. The wind speeds from the land area weather file were between 0.0 m/s and 0.5 m/s considering zero elevation. To simulate the effect of higher wind speed in water bodies an offset of 0.1 m/s is given.

The module area is estimated to be 15.789 ha. Considering a land area multiplier of 1.4 to and an additional land area of 1 ha to accommodate ancillary equipment and walking space the total estimated land area is found to be 39.018 ha or 0.39 km².

4.1 Electrical design

The electrical system for FSPV primarily consists of PV array and inverters. From the California Energy Commission (CEC) database, the Zytech Solar ZT285P polycrystalline silicon modules are selected for PV array and Power electronics: FS1850CU15 inverter module is chosen. Similar electrical configurations are considered for both the land-based PV and floating PV systems. For achievement of 11 MW installed capacity, 5 inverters are chosen. Total 42,068 PV modules (26 modules per strings and 1618 strings in parallel) are required for this purpose. The characteristics of PV module and inverter are shown in the Table 5 and Table 6 respectively. The inverter ratings are chosen to accommodate the maximum string voltage (1180 V_{dc}) and MPP voltage (930.8 V_{dc}) at standard test

Table 4 Parameters for simulation in SAM

Parameters	Data
System nameplate capacity	12,000 kW _{dc}
Module type	Standard
DC to AC ratio	1.1
Rated inverter size (Estimated result)	10,909.09 kW _{ac}
Inverter efficiency	95%
Estimated module area	157,894.737 m ²
Array type	Fixed open rack
Tilt	20°
Azimuth	180°
Ground coverage ratio	0.4

Table 5 Characteristics of PV module

Parameters	Ratings
Number of cells	72
Nominal efficiency	14.78%
Maximum power	285.326 Watt
voltage at maximum power	35.8 V _{dc}
current at maximum power	8.0 A _{dc}
open circuit voltage	45.4 V _{dc}
short circuit current	8.5 A _{dc}

Table 6 Characteristics of Inverter

Parameters	Ratings
Maximum DC power	2.01746 MW _{dc}
Power use during operation	4621.43 W _{dc}
Power use at night	397.3 W _{ac}
Nominal AC voltage	600 V _{ac}
Maximum DC voltage	1200 V _{dc}
Maximum DC current	2146.23 A _{dc}
Minimum MPPT DC voltage	849 V _{dc}
Nominal DC voltage	940 V _{dc}
Maximum MPPT DC voltage	1200 V _{dc}

conditions and maximum DC power for each 2 MW sub-array of PV.

5 Results

For the study area, the average load of the mini micro-grid is estimated to be 1,809.61 kW with a load factor of 55.24% using the typical hourly load variation of rural Jharkhand in Fig. 6 the maximum load at a particular hour is 3,275 kW. The annual energy generation of the FSPV system is 18.08 GWh, which exceeds the annual energy demand of Panchet town and nine nearby villages. The CUF of the FSPV system is found to be 17.2% which is 1.6% more than the equivalent land based PV as shown in Table 7.

The monthly generation of FSPV (E_G) approximately varies between 1.3 GWh and 1.7 GWh as illustrated in Fig. 9. The highest generation occurs in March (1.77 GWh) followed by April (1.73 GWh) and October (1.57 GWh). The lowest generation occurs at July (1.32 GWh) and August (1.38 GWh). The annual energy yield (Y_E) is 1507 kWh/kW which is 10.04% higher than the equivalent land-based PV system. The performance ratio (PR) of the FSPV system is calculated to be 83.4% which is 7.8% higher than

Table 7 Comparison of Land based PV and FSPV system of equal area in Panchet

Metric	Value (Land)	Value (Water)	Percentage increment (%)
E_G (GWh)	16.38	18.08	10.04
DC CUF	15.6%	17.2%	1.6
Y_E (kWh/kW)	1,365	1,507	10.04
$PR(\%)$	83.4	75.6	7.8
E_G in January (GWh)	1.362	1.48989	9.38
E_G in May(GWh)	1.508	1.683	11.60

Table 8 Calculated DSF in different days of the year

Date	Number of hours (H)	$DSF(\%)$
1st January	9	37.5%
1st march	10	41.7%
1st May	11	45.9%
2nd September	6	25.0%

the land-based PV system. The results indicate that lower temperature and high solar irradiation accompanied by good clearness index of the sky are optimal for PV systems.

The statistical distribution of power generation (Fig. 10) indicates probability of getting higher generation in FSPV in comparison with land-based PV. The data points corresponding to FSPV system are shifted towards higher power; hence the cumulative distribution line has lesser slope, compared to land-based PV system. The statistical distribution of module temperature (Fig. 11) shows the

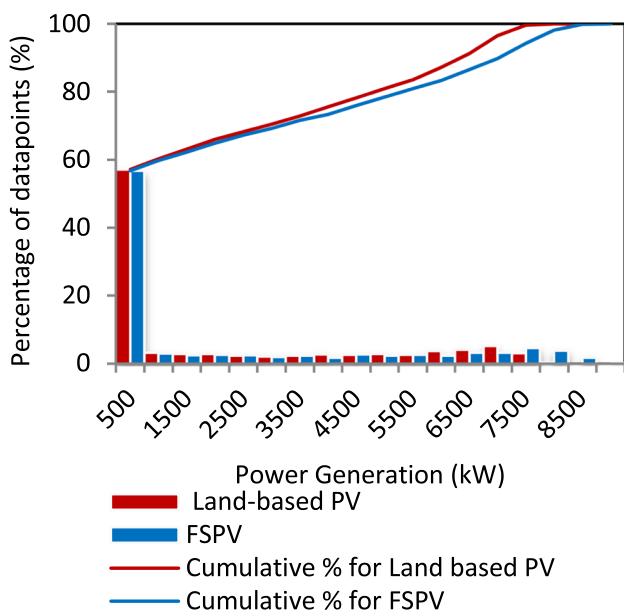


Fig. 10 Statistical distribution of power generation by FSPV and equivalent Land-based PV system

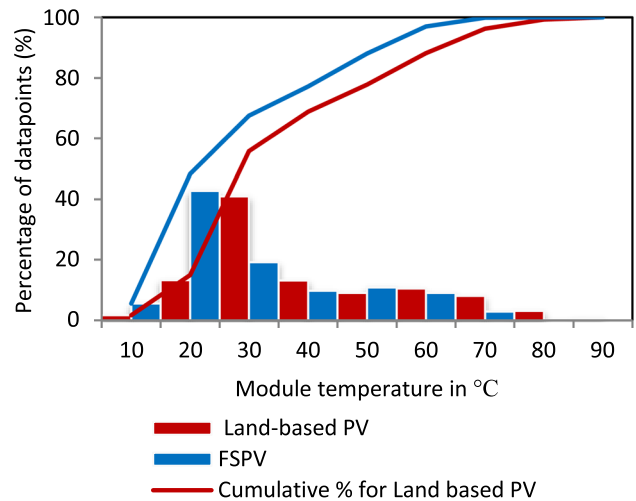


Fig. 11 Statistical distribution of module temperature in FSPV and equivalent Land-based PV system

highest percentage of data points (nearly 40%) between the 20 °C and 30 °C. The data points corresponding to FSPV system are shifted towards lower side, thus limiting the highest module temperature to the range of 75 °C, which is 10 °C cooler compared to the land-based PV system. The improved power output of FSPV system due to decreased temperature is reflected in the statistical distribution of generated power (Fig. 10).

The DSF is the fraction of time when the generation of FSPV system is sufficient to meet the demand. The DSF_{day} is calculated on daily basis for the 1st January, 1st March, 1st May and 2nd September considering the previous hourly load curve as depicted in Table 8. In the Fig. 12, Fig. 13, Fig. 14 and Fig. 15 the green columns indicate the portions where demand is more than generation (therefore grid support is necessary) and the red columns indicate the electricity generation by FSPV system is sufficient to meet the demand. Minimum value DSF_{day} is found to be 2nd September (25%) and the maximum DSF_{day} occurs on 1st May (45.9%).

The RES fraction (F_r) denotes the fraction of load demand catered by the renewable energy sources. The calculated value of F_r for a day in four different seasons

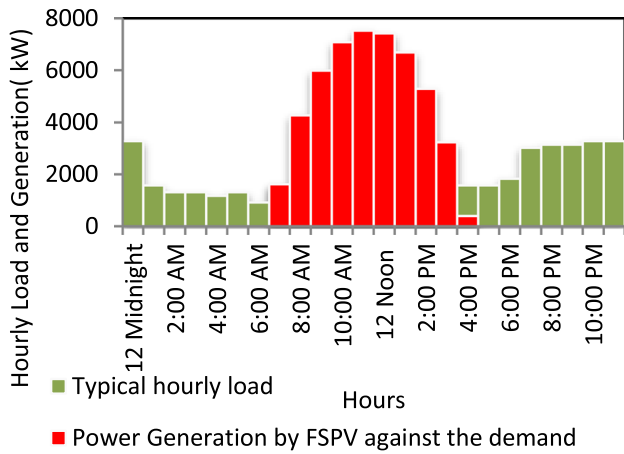


Fig. 12 Hourly demand and power generation by FSPV for calculation of DSF on 1st January

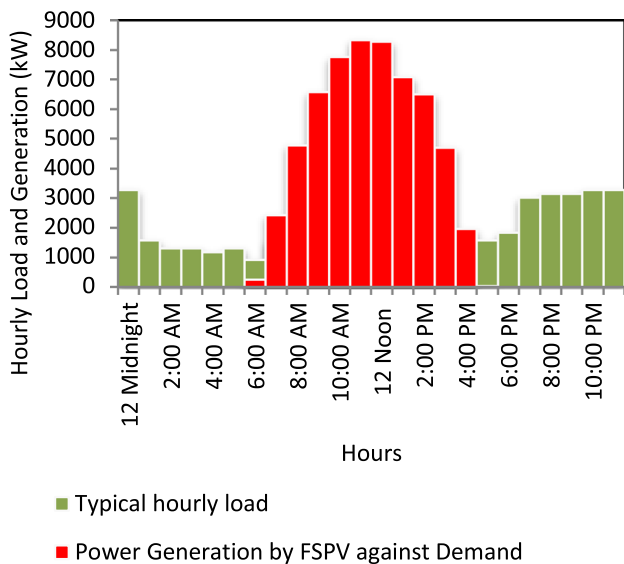


Fig. 13 Hourly demand and power generation by FSPV for calculation of DSF on 1st March

i.e. 1st January, 1st March, 1st May and 2nd September is shown in Fig. 16. From 7 am to 3 pm, F_r is found to be unity for most of the seasons except monsoon.

The DC capacity utilization factor of the FSPV is 17.2%, which is 1.6% higher than the equivalent land-based PV system. The statistical distribution of module temperature in FSPV system is shifted to the lower side. As, the lower module temperature corresponds to higher energy conversion efficiency, the FSPV system has more power generation compared to land-based PV systems.

The seasonal variation of FSPV system performance is evaluated in terms of Demand–Supply-Factor (DSF) and RES fraction (F_r) for four days in winter, spring, summer, and monsoon. The DSF in 1st January, 1st March, 1st May and 2nd September is found to be 37.5%, 41.7%, 45.9%

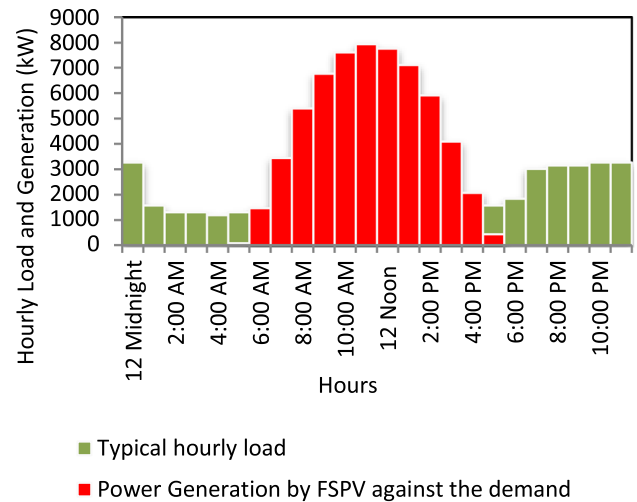


Fig. 14 Hourly demand and power generation by FSPV for calculation of DSF on 1st May

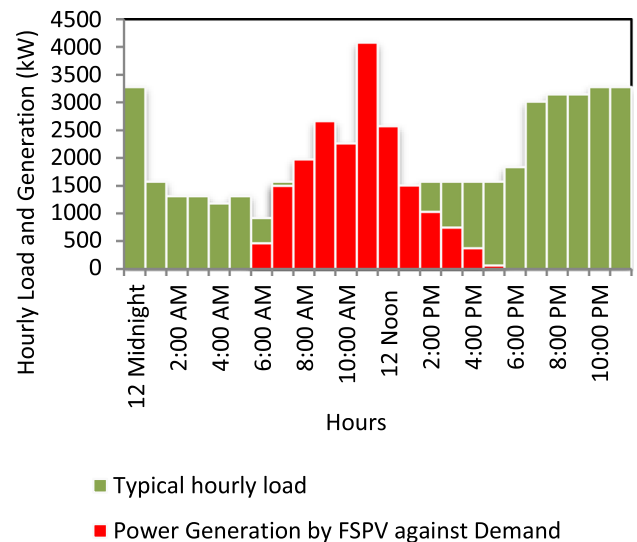


Fig. 15 Hourly demand and power generation by FSPV for calculation of DSF on 2nd September

and 25% respectively. The average value of F_r in 1st January, 1st March, 1st May and 2nd September is calculated to be 0.386, 0.429, 0.472 and 0.369 respectively.

6 Discussions

A FSPV system of 11 MW installed capacity is designed for supplying a mini micro-grid in Panchet census town and nine nearby villages. The maximum available area is chosen in terms of the 80% availability of reservoir water level. 1% of that area has been utilized to cater the demand of rural micro-grid. The requirement of mooring and anchoring design has been evaluated from flood duration

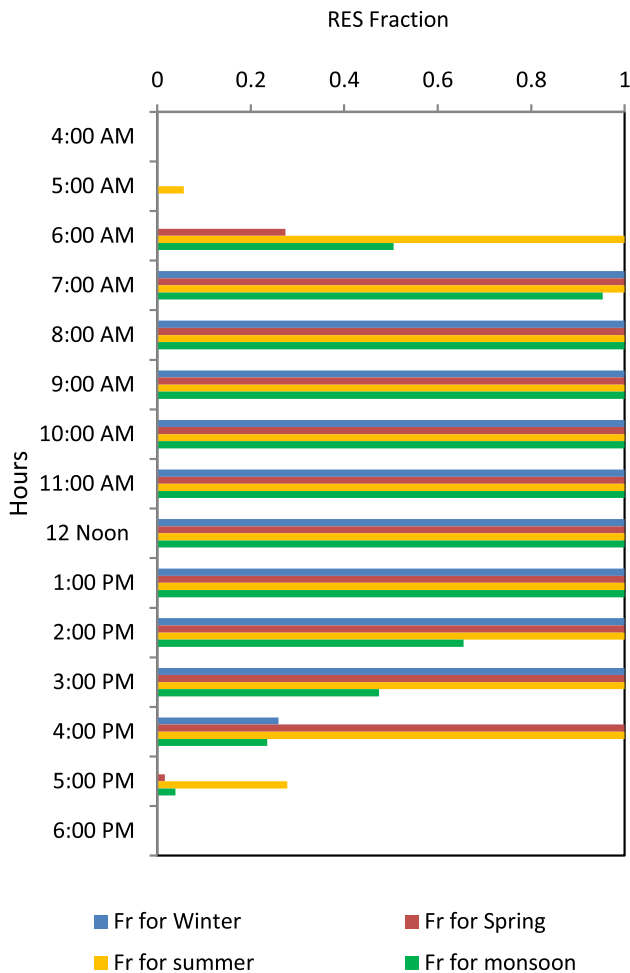


Fig. 16 Hourly variation of RES fraction (F_r) in four seasons

curves where the fluctuation of water level is estimated to be 3 m.

The study area has an annual energy requirement of 15.85 GWh at a load factor of 55.24%. The FSPV system requires total 42,068 PV modules (26 modules per strings and 1618 strings in parallel) and 5 inverters of 2 MW rating. The system with an 11 MW installed capacity annually generates 18.08 GWh, which is 10.03% higher than the equivalent land-based PV system. March experiences the highest monthly generation and July corresponds to the lowest, due to variation in solar irradiation and average temperature. The energy yield is found to be 1507 kWh/kW (10.03% higher than the equivalent land-based PV system). The performance ratio of the FSPV system is calculated to be 83.4% which is 7.8% higher than the land-based PV system. The comparison between statistical distributions of power output in FSPV system and equivalent land-based PV system indicates better utilization of installed capacity for floating solar photovoltaic systems. For the FSPV system with 11 MW installed capacity, 19.20% of the data points have the generation higher than

half of the installed capacity (i.e. 5.5 MW), compared to 16.49% of the datapoints for equivalent land based PV.

7 Conclusion

This paper presents a systematic study on design and development of FSPV system for powering micro-grid with an objective of improving energy security and RES penetration. The selected study area has a lower-than-average but steadily increasing per capita demand; resulting in occasional power outages. The lower share of renewable sources due to overreliance on coal-based-thermal-power plant indicates a remarkable scope of expansion for PV installation. The FDC based sizing methodology has been utilized in designing the FSPV plant. The FSPV system covers less than 1% of the reservoir which indicates that probable ecological impacts of FSPV would be negligible. The FSPV system reliably meets the electricity demand of the region for 9 to 11 h a day, with a small exception of few days in monsoon. The power for rest of the hours is to be supplied by the grid. However, the cost of electricity purchase from the grid is entirely or partially compensated if the excess generation from FSPV in day time is fed to the grid. The results indicate competitive advantages of FSPV over traditional land-based PV systems. This study would help the policy-makers, engineers and academia for planning and implementation of FSPV system as economic, low-carbon and renewable energy sources for sustainable development.

Funding The authors acknowledge the help of Department of Electrical Engineering, IIT (ISM) Dhanbad for offering the necessary facilities to perform the research.

Data availability Not Applicable.

Declarations

Conflict of interest The authors declare that they have no conflict of interest.

Ethical approval This article does not contain any studies with human participants or animals performed by any of the authors.

Informed consent Informed consent is not applicable since human participants were not involved in the study.

References

- Agrawal, S., Bali, N. and Urpelainen, J., (2019) Rural electrification in India: Customer behaviour and demand. *Report, Smart Power India & Initiative for Sustainable Energy Policy*.

- Al-Ghussain L, Samu R, Taylan O, Fahrioglu M (2020) Sizing renewable energy systems with energy storage systems in microgrids for maximum cost-efficient utilization of renewable energy resources. *Sustain Cities Soc* 55:102059. <https://doi.org/10.1016/j.scs.2020.102059>
- Alktrane M, Bencs P (2022) Effect of evaporative cooling on photovoltaic module performance. *Proc Integ Optim Sustain* 6(4):921–930. <https://doi.org/10.1007/s41660-022-00268-w>
- Barron-Gafford GA, Minor RL, Allen NA, Cronin AD, Brooks AE, Pavao-Zuckerman MA (2016) The Photovoltaic heat island effect: larger solar power plants increase local temperatures. *Sci Rep*. <https://doi.org/10.1038/srep35070>
- Central Electricity Authority (CEA) Dashboard. (2020, April 21). Retrieved June 1, 2022, from <https://cea.nic.in/dashboard/?lang=en>
- Central Electricity Authority (CEA). (2022, May). Executive Summary on Power Sector March-2022. Retrieved June 1, 2022, from https://cea.nic.in/wp-content/uploads/executive/2022/03/Executive_Summary_Mar_2022.pdf
- Gadzanku, S, Beshilas L, & Grunwald U. (Bryn) (2021) Enabling Floating Solar Photovoltaic (FPV) Deployment: Review of Barriers to FPV Deployment in Southeast Asia. <https://doi.org/10.2172/1787553>.
- Gonzalez Sanchez R, Kougiass I, Moner-Girona M, Fahl F, Jäger-Waldau A (2021) Assessment of floating solar photovoltaics potential in existing hydropower reservoirs in Africa. *Renew Energy* 169:687–699. <https://doi.org/10.1016/j.renene.2021.01.041>
- Goswami A, Sadhu P, Goswami U, Sadhu PK (2019) Floating solar power plant for sustainable development: a techno-economic analysis. *Environ Prog Sustain Energy*. <https://doi.org/10.1002/ep.13268>
- Goswami A, Sadhu P, Sadhu PK (2020) Development of a Grid connected solar-wind hybrid system with reduction in levelized tariff for a remote Island in India. *J Solar Energy Eng* 142(4):044501
- Green MA (1982) *Solar cells: operating principles, technology, and system applications*. Englewood Cliffs. [https://doi.org/10.1016/0038-092x\(82\)90265-1](https://doi.org/10.1016/0038-092x(82)90265-1)
- Hafeez H, Kashif Janjua A, Nisar H, Shakir S, Shahzad N, Waqas A (2022) Techno-economic perspective of a floating solar PV deployment over urban lakes: a case study of NUST lake Islamabad. *Sol Energy* 231:355–364. <https://doi.org/10.1016/j.solener.2021.11.071>
- IEA (2022) *Renewable energy market update: outlook for 2022 and 2023*. OECD Publishing, Paris. <https://doi.org/10.1787/faf30e5a-en>
- IEA (2021), *World Energy Outlook 2021*, IEA, Paris <https://www.iea.org/reports/world-energy-outlook-2021>
- IISD (2022) *Mapping India's Energy Policy 2022: Aligning support and revenues with a net-zero future*. <https://www.iisd.org/system/files/2022-05/mapping-india-energy-policy-2022.pdf>
- IRENA (2019), *Future of Solar Photovoltaic: Deployment, investment, technology, grid integration and socio-economic aspects (A Global Energy Transformation: paper)*, International Renewable Energy Agency, Abu Dhabi. Retrieved June 1, 2022 <https://www.irena.org/publications>
- IRENA (2022), *Renewable Energy Statistics 2022*, The International Renewable Energy Agency, Abu Dhabi Retrieved June 1, 2022, from <https://www.irena.org/statistics>
- Kiesecker J, Baruch-Mordo S, Heiner M, Negandhi D, Oakleaf J, Kennedy C, Chauhan P (2019) Renewable energy and land use in India: a vision to facilitate sustainable development. *Sustainability* 12(1):281. <https://doi.org/10.3390/su12010281>
- Kjeldstad T, Lindholm D, Marstein E, Selj J (2021) Cooling of floating photovoltaics and the importance of water temperature. *Sol Energy* 218:544–551. <https://doi.org/10.1016/j.solener.2021.03.022>
- Lee N, Grunwald U, Rosenlieb E, Mirletz H, Aznar A, Spencer R, Cox S (2020) Hybrid floating solar photovoltaics-hydropower systems: benefits and global assessment of technical potential. *Renew Energy* 162:1415–1427. <https://doi.org/10.1016/j.renene.2020.08.080>
- Liu L, Wang Q, Lin H, Li H, Sun Q, wennersten, R. (2017) Power generation efficiency and prospects of floating photovoltaic systems. *Energy Procedia* 105:1136–1142. <https://doi.org/10.1016/j.egypro.2017.03.483>
- Makhija SP, Dubey SP, Bansal RC, Jena PK (2021) Techno-environmental analysis of floating PV/On-ground pv/grid extension systems for electrification of a remote area in India. *Technol Econom Smart Grids Sustain Energy*. <https://doi.org/10.1007/s40866-021-00104-z>
- Nag AK, Sarkar S (2018) Modeling of hybrid energy system for futuristic energy demand of an Indian rural area and their optimal and sensitivity analysis. *Renew Energy* 118:477–488. <https://doi.org/10.1016/j.renene.2017.11.047>
- NWIC (2022) *Daily Reservoir Level & Storage Timeseries Timeseries data for period 2016–01–01 to 2022–01–01*. Retrieved June 2, 2022, from <https://nwic.gov.in/data>
- Panchet Population Census 2011 - 2022. (n.d.). Retrieved June 2, 2022, from <https://www.census2011.co.in/data/town/362194-panchet-jharkhand.html>
- Precision Survey Consultancy, (2020) “Sedimentation Survey Report of Panchet Reservoir under NHP” Damodar Valley Corporation <https://nhp.mowr.gov.in>
- Prilliman, M., Stein, J. S., Riley, D., & Tamizhmani, G. (2020, June). Transient weighted moving average model of photovoltaic module back-surface temperature. In 2020 47th IEEE Photovoltaic Specialists Conference (PVSC) (pp. 0490–0497). IEEE.
- Ravichandran N, Ravichandran N, Panneerselvam B (2021) Floating photovoltaic system for Indian artificial reservoirs—an effective approach to reduce evaporation and carbon emission. *Int J Environ Sci Technol* 19(8):7951–7968. <https://doi.org/10.1007/s13762-021-03686-4>
- Reges JP, Carvalho PCM, de Araújo JC, Carneiro TC (2022) Sizing Methodology of Floating Photovoltaic Plants in Dams of Semi-Arid Areas. *J SolEnergy Eng* 144(4):041003
- Shyam B, Kanakasabapathy P (2022) Feasibility of floating solar PV integrated pumped storage system for a grid-connected micro-grid under static time of day tariff environment: a case study from India. *Renew Energy* 192:200–221. <https://doi.org/10.1016/j.renene.2022.04.031>
- Solanki, C. S. (2015). *Solar photovoltaics: fundamentals, technologies and applications*. Phi learning pvt. Ltd.ISBN: 978–81–203–5111.
- Spencer RS, Macknick J, Aznar A, Warren A, Reese MO (2018) Floating photovoltaic systems: assessing the technical potential of photovoltaic systems on man-made water bodies in the continental United States. *Environ Sci Technol* 53(3):1680–1689. <https://doi.org/10.1021/acs.est.8b04735>
- Tsai CT, Muna YB, Lin HY, Kuo CC, Hsiung R (2021) Optimal design and performance analysis of solar power microsystem for mini-grid application. *Microsyst Technol* 27(4):1267–1281. <https://doi.org/10.1007/s00542-018-4213-7>
- Van de Ven D-J, Capellan-Peréz I, Arto I, Cazarro I, de Castro C, Patel P, Gonzalez-Eguino M (2021) The potential land requirements and related land use change emissions of solar energy. *Sci Rep*. <https://doi.org/10.1038/s41598-021-82042-5>
- Villalva MG, Gazoli JR, Filho ER (2009) Comprehensive approach to modeling and simulation of photovoltaic arrays. *IEEE Trans Power Electron* 24(5):1198–1208. <https://doi.org/10.1109/tpele.2009.2013862>

- Wang Y, Kamari ML, Haghghat S, Ngo PTT (2020) Electrical and thermal analyses of solar PV module by considering realistic working conditions. *J Therm Anal Calorim* 144(5):1925–1934. <https://doi.org/10.1007/s10973-020-09752-2>
- Yadav AS, Mukherjee V (2021) Conventional and advanced PV array configurations to extract maximum power under partial shading conditions: a review. *Renew Energy* 178:977–1005. <https://doi.org/10.1016/j.renene.2021.06.029>

Publisher's Note Springer Nature remains neutral with regard to jurisdictional claims in published maps and institutional affiliations.

Springer Nature or its licensor (e.g. a society or other partner) holds exclusive rights to this article under a publishing agreement with the author(s) or other rightsholder(s); author self-archiving of the accepted manuscript version of this article is solely governed by the terms of such publishing agreement and applicable law.